Ecological Informatics 63 (2021) 101300

Contents lists available at ScienceDirect

Ecological Informatics

journal homepage: www.elsevier.com/locate/ecolinf

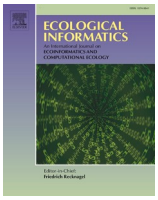

A new approach of deep neural computing for spatial prediction of wildfire danger at tropical climate areas

Hung Van Le [a,*], Duc Anh Hoang [a], Chuyen Trung Tran [a], Phi Quoc Nguyen [b], Van Hai Thi Tran [a], Nhat Duc Hoang [c,d], Mahdis Amiri [e], Thao Phuong Thi Ngo [a], Ha Viet Nhu [f], Thong Van Hoang [g], Dieu Tien Bui [h]

[a] Faculty of Information Technology, Hanoi University of Mining and Geology, Duc Thang, Bac Tu Liem, Hanoi, Viet Nam
[b] Department of Environmental Sciences, Hanoi University of Mining and Geology, Duc Thang, Bac Tu Liem, Hanoi, Viet Nam
[c] Institute of Research and Development, Duy Tan University, Da Nang, 550000, P809 - 03 Quang Trung, Viet Nam
[d] Faculty of Civil Engineering, Duy Tan University, Da Nang, 550000, P809 - 03 Quang Trung, Viet Nam
[e] Gorgan University of Agricultural Sciences & Natural Resources, Department of Watershed & Arid Zone Management, Gorgan, Iran
[f] Department of Geological-Geotechnical Engineering, Hanoi University of Mining and Geology, Hanoi, Viet Nam
[g] Information Technology Faculty, University of Transport and Communications, Hanoi, Viet Nam.
[h] GIS Group, Department of Business and IT, University of South-Eastern Norway, Gullbringvegen 36, N-3800, Bø i Telemark, Norway

ARTICLE INFO

Keywords:
Forest fire
Deep neural computing
Optimization algorithm
Geographical information system
Gia Lai
Vietnam

ABSTRACT

Wildfire is an environmental hazard that has both local and global effects, causing economic losses and various severe environmental problems. Due to the adverse effects of climate changes and anthropogenic activities, wildfire is anticipated more frequent and extreme; therefore, new and more efficient tools for forest fire prevention and control are essential. This study proposes a new deep neural computing approach for spatial prediction of wildfire in a tropical climate area. For this purpose, deep neural computing (Deep-NC) with a structure of 3 hidden layers was proposed. The Rectified Linear Unit (ReLU) activation function was adopted to infer wildfire dangers from the input factors. To search and optimize the weights of the model, Stochastic Gradient Descent (SGD), Root Mean Square Propagation (RMSProp), Adaptive Moment Estimation (Adam), and Adadelta optimizers were employed. Also, this study has established a Geographic Information System (GIS) database for Gia Lai province (Vietnam) to train and verify the newly developed deep computing approach. The twelve ignition factors, namely, slope, aspect, elevation, curvature, land use, NVDI, NDWI, NDMI, temperature, wind speed, relative humidity, and rainfall, have been used to characterize the study area with respect to forest fire susceptibility. According to experimental results, the Adam optimized Deep-NC model delivered the highest predictive accuracy (AUC = 0.894, Kappa = 0.63). Accordingly, this model has been employed to establish a forest fire susceptibility map for Gia Lai province. The proposed Deep-NC model and the newly constructed forest fire susceptibility map can help local authorities in land use planning and hazard mitigation/prevention.

1. Introduction

Wildfires are mostly unplanned vegetation ignitions, which can happen in forests, bushes, grassland, and other ecosystem areas (Gill et al., 2013). Although fires are vital components for maintaining the natural systems (Chuvieco et al., 2010a), in tropical areas, they may become destructive and unpredictable (Taufik et al., 2017; Wibisana, 2019), i.e., fires occurring near populated areas without control (Barrera et al., 2018). In recent years, climate and weather conditions have become critical factors for wildfire occurrences in various areas (Lozano et al., 2017; Pereira et al., 2020). It is anticipated that wildfires will be more frequent and extreme in many areas due to changes in climate and anthropogenic activities (Opitz et al., 2020); therefore, it is essential to develop preventive measures for forest protection and management. In this context, accurately predicting wildfire and understanding its critical factors are crucial (Çolak and Sunar, 2020a; Di Virgilio et al., 2019;

* Corresponding author.
E-mail addresses: levanhung@humg.edu.vn (H.V. Le), hoanganhduc@humg.edu.vn (D.A. Hoang), trantrungchuyen@humg.edu.vn (C.T. Tran), nguyenquocphi@humg.edu.vn (P.Q. Nguyen), tranthihaivan@humg.edu.vn (V.H.T. Tran), hoangnhatduc@duytan.edu.vn (N.D. Hoang), ngothiphuongthao@humg.edu.vn (T.P.T. Ngo), nhuvietha@humg.edu.vn (H.V. Nhu), thonghv@utc.edu.vn (T.V. Hoang), dieu.t.bui@usn.no (D. Tien Bui).

https://doi.org/10.1016/j.ecoinf.2021.101300
Received 11 June 2020; Received in revised form 5 April 2021; Accepted 5 April 2021
Available online 13 April 2021

Gibson et al., 2020; Mhawej et al., 2015; Mhawej et al., 2016).

Since wildfires have both local and global effects, various models and tools have been developed for wildfire prevention and control strategy worldwide (Akinola and Adegoke, 2019; Chuvieco et al., 2010b; Chuvieco et al., 2014; Çolak and Sunar, 2020b; Hernandez-Leal et al., 2006; Matin et al., 2017; McFayden et al., 2020; Pourghasemi et al., 2020; You et al., 2017). Chuvieco et al. (2014) provided detailed discussions of the fire prevention strategy, including definitions of fire vulnerability, fire hazard, fire risk, and fire danger. The last one should consider various driving factors such as climatic conditions, influencing agents, and possible damages. In other words, the fire danger should provide both spatial and temporal aspects of wildfire as well as its impact. Herein, the spatial prediction of wildfire danger, which is also called wildfire danger susceptibility mapping, is considered one of the most crucial tasks.

With the rapid development of machine learning (ML) and the availability of remote sensing data (Koubarakis et al., 2017; Soille et al., 2018), various advanced statistical and ML models have been developed for spatial prediction of wildfire danger. Herein, machine ML provides new and powerful algorithms (LeCun et al., 2015; Zdeborová, 2017) for inferring a danger index value from a set of input data, whereas the remote sensing technology provides rapid multi-source essential data, i.e., Landsat 8, Sentinel 1 and 2, VIIRS, and MODIS (Claverie et al., 2018; Liu et al., 2017; Mondal et al., 2020; Roy et al., 2019; Teodoro and Amaral, 2019) for deriving both wildfire locations and driving factors. Consequently, ML algorithms have been a hot trend for studying wildfire danger in the last decade, such as, to name a few, Chuvieco et al. (2014) integrated geospatial information and geographically weighted regression for forest fire assessment in Spain. The result showed a significant correlation ($R^2 = 0.7$) between the fire danger map and the fire occurrence. Guo et al. (2016a) employed logistic regression, Ripley's K-function, and geospatial information system (GIS) data for analysis of the spatial pattern of forest fires in China. The performance of the models was between 80% and 90%. Tehrany et al. (2019) used multi-source geospatial data and ensemble ML for predicting tropical forest fires in Vietnam. The highest performance (92%) belonged to the LogitBoost ensemble tree model. In recent work, Naderpour et al. (2019) summarized studies from 2000 to 2018 on forest fires using geospatial data, statistical methods, multi-criteria techniques, ML and ensemble algorithms with the report that, the last group is capable of delivering the highest accuracy. Therefore, the exploration of new ML algorithms for forest fire modeling is essential.

Deep learning models have been proposed and proven to outperform both traditional methods and popular ML algorithms in various domains (Bolton and Zanna, 2019; Jiang et al., 2018; Ross et al., 2019; Silva et al., 2019). Deep learning, which is a sub-branch of ML, refers to learning processes with the use of "deep" neural network structures to infer outcomes from a set of input variables. Famous deep structures can be named a few, such as deep convolutional neural networks (CNN), deep learning neural networks (DLNN), and deep recurrent neural networks (RNN). A review of deep learning algorithms can be found in Guo et al. (2016b). In the field of forest fire evaluation, several attempts have been carried out with promising results, including exploration of reinforcement learning for spreading of forest fires (Ganapathi Subramanian and Crowley, 2018), investigations of CNN for forest fire susceptibility mapping (Zhang et al., 2019), smoke detections (Peng and Wang, 2019), and forest fire detections (Wang et al., 2019).

Nevertheless, to our knowledge, an exploration of DLNN for forest fire susceptibility mapping has seldom been carried out. Thus, the aim of this work is to partially fill this gap in the literature by investigating the potential applicability of the GIS-based Deep-NC model for susceptibility mapping of forest fires. Herein, multiple optimization methods for Deep-NC are utilized. More concretely, Stochastic Gradient Descent (SGD), Root Mean Square Propagation (RMSProp), Adaptive Moment Estimation (Adam), and Adadelta optimizers are employed. The tropical forest of Gia Lai province in the Central Highland of Vietnam was selected as a case study to train and verify the models. This province has particularly faced the forest fire problem during the last ten years. Notably, this is one of the most sensitive provinces affected by the El Niño Southern Oscillation that caused severe droughts and forest fires in 2016 (CGIAR, 2016). The subsequent sections of the article are organized as follows: The second section reviews the background of the employed method. The next part provides a general description of the study area. The proposed Deep-NC used for deriving the forest fire susceptibility is presented in the fourth section. The fifth section reports the experimental results of the study, followed by concluding remarks stated in the final section.

2. Background of the algorithms used

2.1. Deep neural computing

One of the most important benefits of deep learning is the independent extraction of discriminatory features from raw data (Heaton, 2015). Deep learning has been used successfully in various applications, including spatial mapping of natural hazards (Nhu et al., 2020; Sankaranarayanan et al., 2020; Wu et al., 2020; Zhang et al., 2019). On the other hand, deep learning is a multi-level representational learning method that is achieved by composing nonlinear but straightforward modules that transform each representation on a single level (LeCun et al., 2015). By representing at a high level with an increasing degree of abstraction and combining such transformations sufficiently, a deep learning model can generalize very complex mapping functions. Particularly for classification tasks, the higher layers represent the input aspects that are important for discrimination and reinforce the suppression of irrelevant changes.

Usually, a deep learning architecture consists of the following layers: one input layer, a number of hidden layers, and one output layer (refer to Fig. 1). The number of hidden layers determines the depth of the architecture. Depending on the type of hidden layers used, different nonlinear mapping functions can be learned by adapting the deep neural network structure (Singaravel et al., 2018). Fig. 1 presents a typical deep neural network architecture feasibly used for spatial mapping of forest fire danger. The input layer provides vectors of raw features that are used to describe the natural conditions (e.g., slope and rainfall) and human activity-related conditions (e.g., land use). The hidden layers progressively process the input information and create abstractions so that complex concepts can be learned more easily. In the final layer, the softmax activation function can be employed to derive the output class probabilities (Kim, 2017; Skansi, 2018). Herein, there are two output classes of "non-forest fire" and "forest fire", in terms of probability indices. The probability indices of the forest fire will be used to generate a forest fire danger map.

2.2. Optimization algorithms

It is noted that Deep-NC models are able to perform high-level feature extraction during the training process autonomously (Hoang et al., 2018a). This high-level feature extraction is achieved via self-adaptions of the weights within the hidden layers of the models (Sugomori et al., 2017).

It is notable that the capability of inferring high-level representations of the original features can be considered as a major advantage of this advanced ML method. Nevertheless, the capability of the high-level feature extraction in deep neural networks primarily depends on the optimization algorithms used for fine-tuning the networks' weights. The process of weight adaptation is illustrated in Fig. 2. Herein, the well-known optimizers, namely, Stochastic Gradient Descent (SGD), Root Mean Square Propagation (RMSProp), Adaptive Moment Estimation (Adam), and Adadelta are reviewed.

2.2.1. Stochastic gradient descent (SGD)

Using the conventional batched gradient descent approach, the network weight (w) is adapted using Eq. (1) (Kim, 2017):

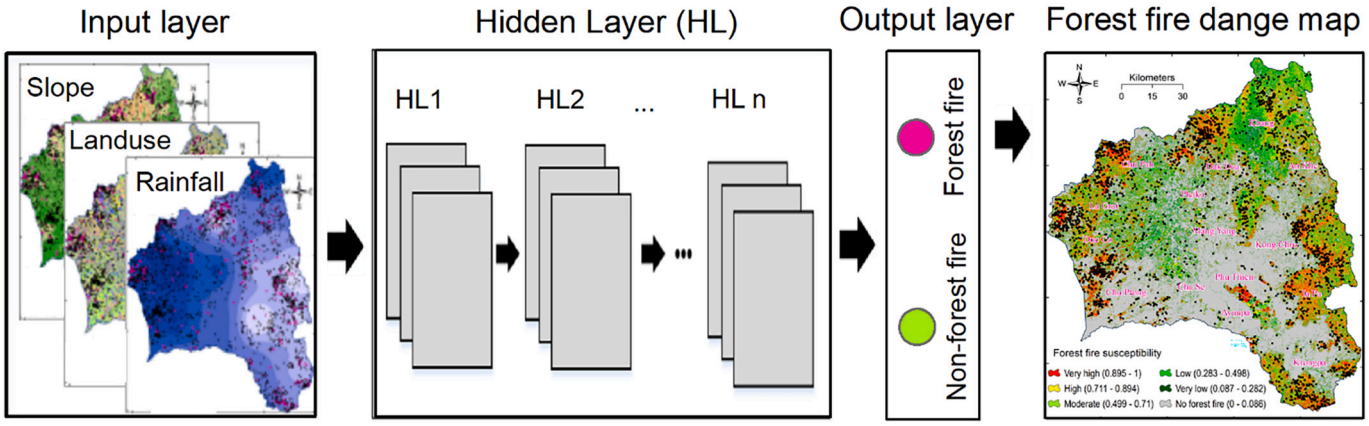

Fig. 1. The general structure of a deep learning model.

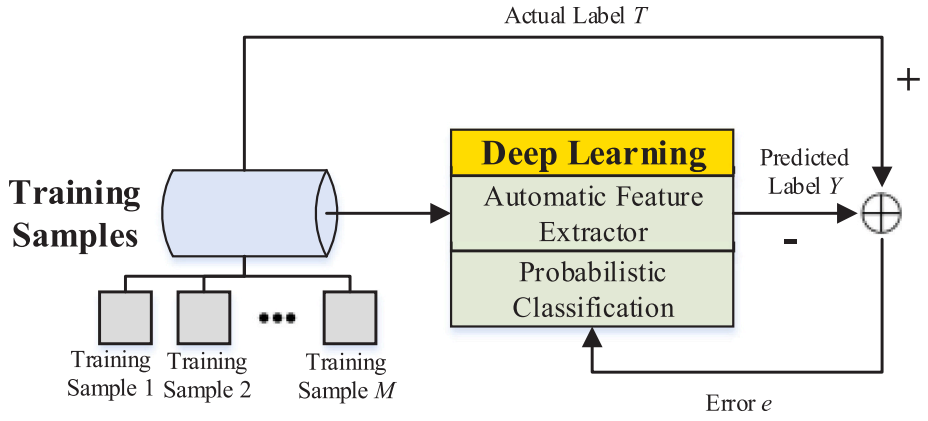

Fig. 2. The general process of network weight adaptation.

$$w = w - \alpha \nabla L(w) \tag{1}$$

where α denotes the learning rate parameter;∇L is the gradient

The batched gradient descent algorithm has been proved to converge to the global minimum for convex loss functions and a local minimum for non-convex ones (Goodfellow et al., 2016). Nevertheless, one major disadvantage of the conventional batched gradient descent is that the component gradient ∇L_i for each sample in the dataset must be computed entirely. This fact can lead to a high computational expense for large-sized training datasets. In order to improve the performance of the batched gradient descent algorithm, stochastic gradient descent (SGD) is proposed (Goodfellow et al., 2016).

The SGD is considered as a stochastic approximation of gradient descent optimization because it substitutes the actual gradient by an approximation gradient via sub-sampling of the whole training data. The equation used for updating the deep model's weights is presented in Eq. (2).

$$w = w - \alpha \nabla L_i(w) \tag{2}$$

2.2.2. Root mean square propagation (RMSProp)

The RMSProp has been proposed by Tieleman and Hinton (2012), and it is designed to reduce the oscillating phenomenon via the employment of lessened learning rates for updating oscillating weights. Networks' weights that are not subject to oscillating phenomena are updated with larger learning rates. Tieleman and Hinton (2012) introduced the concept of learning rate (α) scaling via the use of the term of $\nu_t^{(j)}$ which is the exponentially weighted moving average of squares of the associated gradients (partial derivatives), $g_t^{(j)}$(Nhu et al., 2020). Eqs. (3) and (4) used for updating weights are described as follows:

$$\nu_t^{(j)} = \rho \nu_{t-1}^{(j)} + (1-\rho)\left(g_t^{(j)}\right)^2 \tag{3}$$

$$w_{t+1}^{(j)} = w_t^{(j)} - \frac{\alpha}{\sqrt{\nu_t^{(j)} + \varepsilon}}\, g_t^{(j)} \tag{4}$$

where t is the step in the SGD optimizer; j represents the associated component weight; ρ denotes a hyper-parameter of the algorithm (ρ of 0.9 can be a good initial start); $\varepsilon = 10^{-8}$ denotes a small positive number used to avoid division by zero.

2.2.3. Adaptive moment estimation (Adam)

The Adam optimizer, first proposed by Kingma and Ba (2015a), Kingma and Ba, 2015b), has the feature of fine-tuning the learning rates for each network weight automatically. Moreover, this method uses a record of an exponentially decaying average of past squared gradients. The Adam can be considered as an integration of the aforementioned SGD and RMSprop algorithms.

Besides the term $\nu_t^{(j)}$ (regarded as the second moment) used similarly in the RMSProp optimizer, the Adam algorithm calculates the momentum (regarded as the first moment) as the exponentially weighted average of gradients (Nhu et al., 2020):

$$m_t^{(j)} = \beta_1 m_{t-1}^{(j)} + (1-\beta_1) g_t^{(j)} \tag{5}$$

$$\nu_t^{(j)} = \beta_2 \nu_{t-1}^{(j)} + (1-\beta_2)\left(g_t^{(j)}\right)^2 \tag{6}$$

where the hyper-parameters β_1 and β_2 are recommended to be 0.9 and 0.999, respectively (Kingma and Ba, 2015a; Kingma and Ba, 2015b).

Accordingly, the first and second moments are computed using Eq. (7).

$$\widehat{m}_t^{(j)} = \frac{m_t^{(j)}}{1-\beta_1^t}, \widehat{\nu}_t^{(j)} = \frac{\nu_t^{(j)}}{1-\beta_2^t} \tag{7}$$

Finally, the deep neural network's weights are adapted using Eq. (8):

$$w_{t+1}^{(j)} = w_t^{(j)} - \frac{\alpha}{\sqrt{\widehat{\nu}_t^{(j)}} + \varepsilon}\widehat{m}_t^{(j)} \tag{8}$$

2.2.4. Adadelta optimizer

The Adadelta, first proposed by Zeiler (2012), is an advanced optimizer that aims at alleviating the phenomenon of monotonically decreasing the learning rate (Ruder, 2017). To achieve this purpose, this optimizer confines the window of accumulated past gradients to a certain fixed size. It is also noted that the Adadelta method does not require the setting of a default learning rate. The equations used to update the network's weights are presented in Eq. (9).

$$w_{t+1}^{(j)} = w_t^{(j)} - \frac{RMS[\Delta w]t}{RMS[g]t} g_t^{(j)} \tag{9}$$

where RMS denotes the root mean squared error of the parameter updates (Zeiler, 2012).

3. The study area and GIS database

3.1. Description of the study area

Gia Lai province is situated in the south-central region of Vietnam, covering an area of 15,512 km^2. Topographically, the highest altitude is 1748 m at Kon Ka Kinh mountain, which belongs to K'Bang district, whereas the lowest altitude is 80 m at Krongpa district. The total population of the province is 1,513,847 people in 2019, with the population density of 94 people/km^2 (GSO, 2019).

Regarding the economy of the province, according to the statistical yearbook of Vietnam 2018 (General Statistic Office, 2018), agriculture, forestry, and fishing accounted for 32.75% of the Gross Domestic Product (GDP). In contrast, industry and construction were 27.81%, and services were 35.96%. In 2018, around 93.13% was agriculture and forestry lands, whereas residential land was 1.22%. The total forest area was 632,200 ha, which accounts for 40.8% of the total study area. The areas with natural forest and planted forest were 5436 ha and 88,600 ha, and they account for 35.04% and 5.71% of the total area of the province, respectively (General Statistic Office, 2018).

The province (Fig. 3) belongs to the tropical monsoon highland climate, with abundant humidity and a high amount of rainfall (Van et al., 2014). The climate is separated clearly into two distinct seasons: dry and rainy seasons. The rainy season usually starts in May and ends in October, whereas the dry season is from November to April in the following year. The annual average temperature is from 22 to 25 °C, whereas the annual average precipitation is 2100–2200 mm.

Regarding wildfire, this province has been suffering from this hazard for the last ten years (Le et al., 2020). According to the department of forest protection of the province, currently, more than 270,000 ha of forest is highly sensitive to fire. Only in the first four months in 2020, two severe wildfire events occurred, namely, the fire occurred at the protective forest area of Ham Rong-Plei Ku destroying 2 ha of forest and the fire happened at Ia Grai district from April 4 to 9 destroying 17 ha of pine forest.

3.2. Wildfire data

The wildfire modeling using Deep-NC in this work is of supervised learning, where the model uses the data of historical forest fire locations (Fig. 3), and the inputs are ignition factors. Therefore, the collection of historical forest fires with high accuracy is a key task. In this research, a forest fire database, which consists of 2530 historical fire locations occurring during 2007–2016, prepared by Le et al. (2020) was used. These fire locations were derived from the fire database provided by the Ministry of Agriculture and Rural Development (MARD) of Vietnam and available at http://www.kiemlam.org.vn.

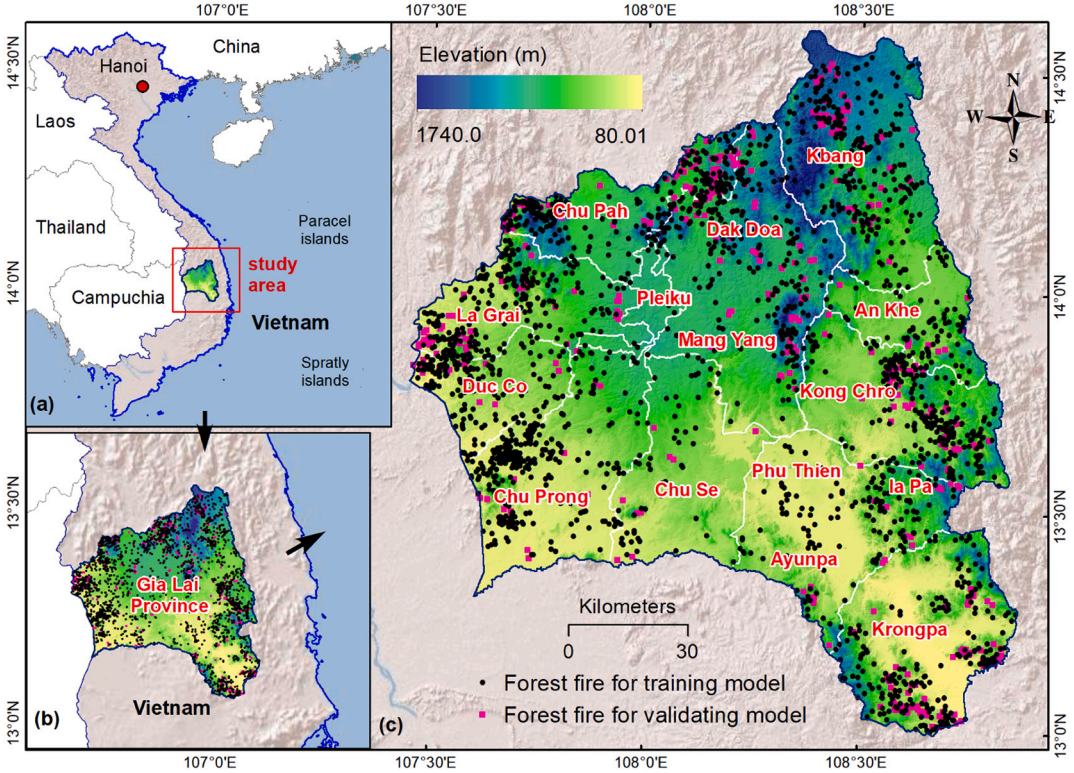

Fig. 3. (a) and (b) Location of Gia Lai province in Vietnam; and (c) Gia Lai province and forest fire locations map.

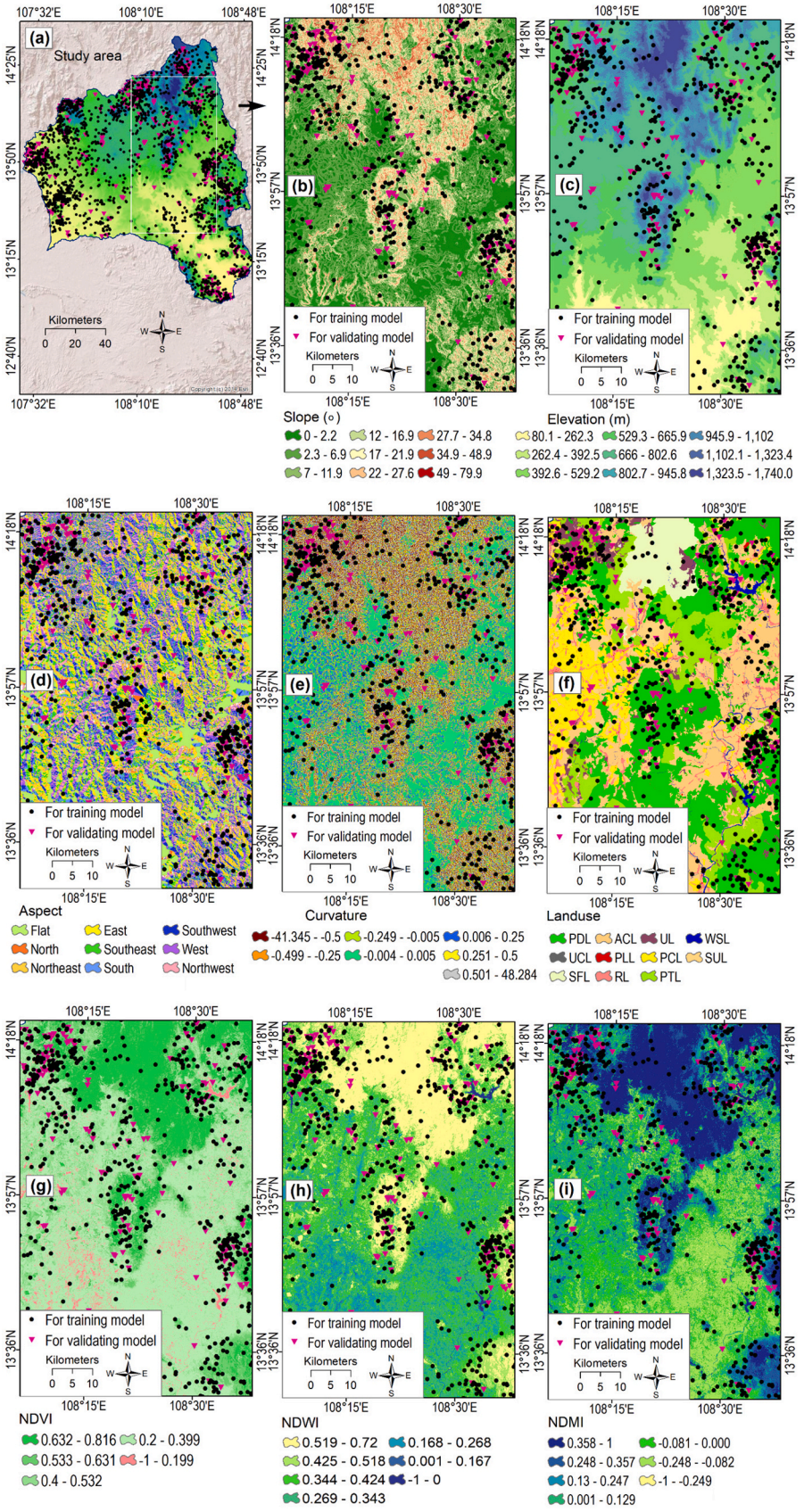

Fig. 4. Forest fire ignition factors used in this study: (a) Overview map of Gia Lai province; (b) Elevation map; (c) Slope map; (d) Aspect map; (e) Curvature map; (f) Land use map; (g) NDVI map; (h) NDWI map; (i) NDMI map; (j) Temperature map; (k) Wind speed map; (l) Relative humidity map; and (m) Rainfall map.

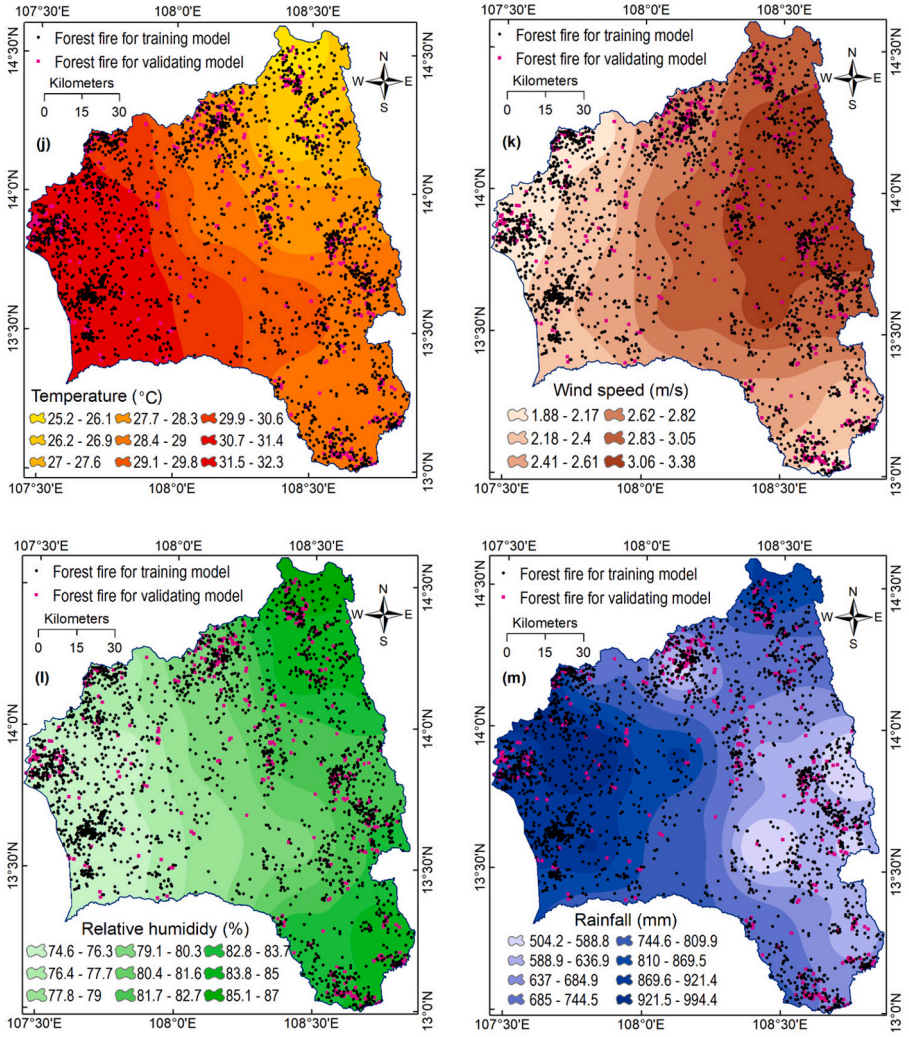

Fig. 4. (*continued*).

Our statistical analysis showed that around 90% of these fires occurred in the dry months from January to May. Forest fires severely occurred in 2010, 2013, 2015, and 2016, which were strongly affected by the El Niño–Southern Oscillation (ENSO) activities causing prolonged droughts in the province. Herein, the rainfall was around 12% lower than that of average years (Sutton et al., 2019). In contrast, almost no fire was reported in years with La Nina events, e.g., 2011.

3.3. Driving factors

The occurrence of wildfire and its spreading have proven to be the result of various interactions of ignition sources and several factors, including topography, fuels, and climate patterns (Cary et al., 2009; Thach et al., 2018); therefore, the determination of driving factors is a crucial task in forest fire modeling. This section provides an overview of the driving factors used in this project. More descriptions of these factors can be found in Le et al. (2020).

3.3.1. Topographical factors

Topography influences both the indirect and direct behavior of wildfires. The variation of topography in a large area can create different local climates, which relate to the temperature, land covers, and the distribution of tree species (Mermoz et al., 2005); therefore, it influences wildfires indirectly. Besides, the topography affects wildfires directly by accelerating the fire transfer in slope directions (Moreno et al., 2014). In this project, a 30 m-resolution digital elevation model (DEM) for Gia Lai province was generated using the 1:50,000 scale topographic maps provided by the Ministry of Natural Resource and Environment (MONRE) of Vietnam. Then, four topography-related factors were generated: elevation (Fig. 4b), slope (Fig. 4c), aspect (Fig. 4d), and curvature (Fig. 4e).

Terrain slope affects the spreading rate of fires directly (Dupuy and Maréchal, 2011), while aspect is related to solar radiation, temperature, wind speed, humidity, and vegetation that are important driving factors of wildfires (Bennie et al., 2008; Johansson et al., 2017). Therefore, both slope and aspect should be selected for wildfire modeling. Terrain elevation affects not only air temperature and humidity but also rainfalls and distributions of plant species (Brunello et al., 2019; Chen et al., 2018); therefore, it should be considered as a driving factor for wildfire study. Regarding the curvature, this factor has proven to be a factor for the propagation of wildfires (Hilton et al., 2017), in which the higher is the local curvature, the faster is the fire spreading.

3.3.2. Anthropogenic and environmental factors

In both developed and developing countries, human activity is considered a leading cause of wildfires. Thus, due to population growth, anthropic pressures on natural resources lead to deforestation and intensification of land use, generating higher wildfire probabilities in some tree species (Kissinger et al., 2019; Viedma et al., 2017). Therefore, land use is an essential factor and should be considered for wildfire modeling. In this research, a land use map (Fig. 4e) with eleven groups

was compiled from the national land use map at a scale of 1: 50,000 provided by MONRE.

Regarding the normalized difference vegetation index (NDVI), this is an indicator of the health status of vegetations (Carlson and Ripley, 1997; Gamon et al., 1995), which relates to the fuel for wildfire; therefore, NDVI (Fig. 4g) was selected in this analysis. In addition to NDVI, the normalized difference water index (NDWI) (Fig. 4h) and the normalized difference moisture index (NDMI) (Fig. 4i) were also considered for the wildfire study because NDWI is an indicator of the water content in the trees, while NDMI is a proxy for the fuel moisture, which influence the behavior of wildfires.

For this project, Landsat-8 OLI images with a 30 m resolution (acquired in 2016 at http://earthexplorer.usgs.gov) were used to compute NDVI (Tucker, 1979), NDWI (McFeeters, 1996), and NDMI (Wilson and Sader, 2002). It should be noted that the images have been calibrated into the Bottom of Atmosphere (BOA) values (surface reflectance values).

$$\text{NDVI} = (\text{NIR band} - \text{Red band})/(\text{NIR band} + \text{Red band}) \tag{10}$$

$$\text{NDWI} = (\text{Green band} - \text{NIR band})/(\text{Green band} + \text{NIR band}) \tag{11}$$

$$\text{NDMI} = (\text{NIR band–SWIR band})/(\text{NIR band} + \text{SWIR band}) \tag{12}$$

where NIR is the near-Infrared band, and SWIR is the Short-wave Infrared band.

3.3.3. Climate factors

Climate change has proven to interlink with the wildfire regimes significantly (Lacroix et al., 2020); therefore, climate-related factors should be used. In this project, four climatic factors, namely, temperature, wind speed, relative humidity, and rainfall, were selected, as their data were available for the study area. In this analysis, the temperature map (Fig. 4j), the wind speed map (Fig. 4k), relative humidity map (Fig. 4l), and the rainfall map (Fig. 4m), which was prepared by Le et al. (2020) was used. Herein, these maps were compiled using the weather data from 2007 to 2014 (available at https://www.ncdc.noaa.gov/).

Temperature is selected because it affects soil moisture and is directly related to the combustion of plants (Pourtaghi et al., 2016). Besides, the rising temperature also affects humidity and forest health, reducing the moisture content of the vegetation (Gillett et al., 2004), and therefore, causing developments of fires. Wind speed is used because it affects the spread of wildfires directly (Alexandridis et al., 2008). Also, wind speed could influence the fuel moisture, provide extra oxygen, and accelerate combustion. Regarding relative humidity and rainfall, they influence fuel moisture (Liu et al., 2013), which is a critical indicator for the ignition of wildfire.

4. The deep-NC methodology

This section describes in detail the proposed approach in this research. It should be noted that the processing of the wildfire data and 12 driving factors was carried out using ArcGIS 10.6. Besides, the Deep-NC model was programmed by the authors in Python environment using the Keras Python deep learning API (Chollet, 2018). Moreover, the authors developed a Python tool to transform the predicted wildfire results into a raster map in ArcGIS. In the Python tool, the ASCII to raster in a geographic information system (Brown, 2014) was employed.

4.1. Wildfire database

Because the proposed Deep-NC used for spatial prediction of forest fire susceptibility is fundamentally a supervised learning method, it is required to establish a GIS database to train the model. The GIS database should include information regarding forest fire inventory and the affecting factors. The fire ignition factors consist of slope, aspect, elevation, curvature, land use, NDVI, NDWI, NDMI, temperature, wind speed, relative humidity, and rainfall. The constructed GIS database used in this study is illustrated in Fig. 5.

Since the concept of the binary pattern GIS-based modeling (Bui et al., 2017) was employed in this research, which requires both forest fire and non-forest fire samples, a total of 2530 non-forest fire data points were randomly sampled from non-forest areas of the study area. Thus, the total number of samples used to train and verify the proposed Deep-NC was 5060. The whole data set was then randomly divided into two mutually exclusive sets: a training set (70%) and a testing set (30%).

It is noted that the GIS database used for forest fire susceptibility mapping consisting of the 12 ignition factors and the fire inventory has been compiled in the ArcGIS 10.6 using the ESRI file geodatabase format. As mentioned earlier, the dataset consists of 5060 data points. Furthermore, regarding data normalization, the data of the influencing factors have been converted from categorical classes into real-valued numbers within the range of 0.01 and 0.99 (Bui et al., 2012).

4.2. Assessment of the predictive importance of the driving factors

In order to have an overview of the wildfire driving factors before going further to wildfire modeling using the deep learning approach, the predictive importance of these factors was assessed. This is because the 12 driving factors were just heuristically selected based on the wildfire data analysis and literature review. In environmental modeling using ML, especially deep learning, it is reasonable to say that some factors may exist noises that could reduce the prediction capability of the wildfire model. Therefore, the predictive importance of these factors should be assessed. In this research, the average impurity decrease (AVID) (Hoa et al., 2019) was used to quantify all factors' predictive importance. When ranking these factors, the AVID method also considered interactions between them. As a result, a factor with a zero AVID value should be removed from the modeling process.

4.3. Objective function for training the deep-NC model

The Deep-NC model training is a process of searching and updating weights of the model to minimize the difference between the predicted wildfires and the actual wildfires. In order to measure this difference, an objective function should be used. In this work, Mean Squared Error (MSE) objective function was selected Eq. (13).

$$L(y, \hat{y}) = \frac{1}{N}\sum_{i=1}^{N}\left(y_i - \hat{y}_i\right)^2 \tag{13}$$

where N denotes the number of data samples; $y_i, \hat{y}_i$ represent the actual and predicted output for sample i, respectively.

4.4. Training and validating the deep-NC model

Based on the training samples and ground truth labels obtained from the constructed GIS database, the Deep-NC model for spatial prediction of forest fire susceptibility mapping can be trained. The overall structure of the deep neural network employed in this study is provided in Fig. 6. The deep neural network consists of an input layer (with 12 input neurons to receive signals of the 12 forest fire influencing factors), a number of hidden layers, and an output layer that returning two-class outputs. The network consists of three hidden layers; each layer has 64 neurons. The rectified linear unit (ReLU) activation function (Goodfellow et al., 2016) is employed for the neurons in the hidden layers.

In order to optimize the weights of the Deep-NC model, SGD, RMSProp, Adam, and Adadelta optimizers are employed. Using the Deep-NC model, a decision boundary that divides the study area's map into two separate categories of "non-forest fire" and "forest fire" can be generated. Subsequently, the Deep-NC prediction outcomes can be transformed into a raster format and analyzed by the ArcGIS package.

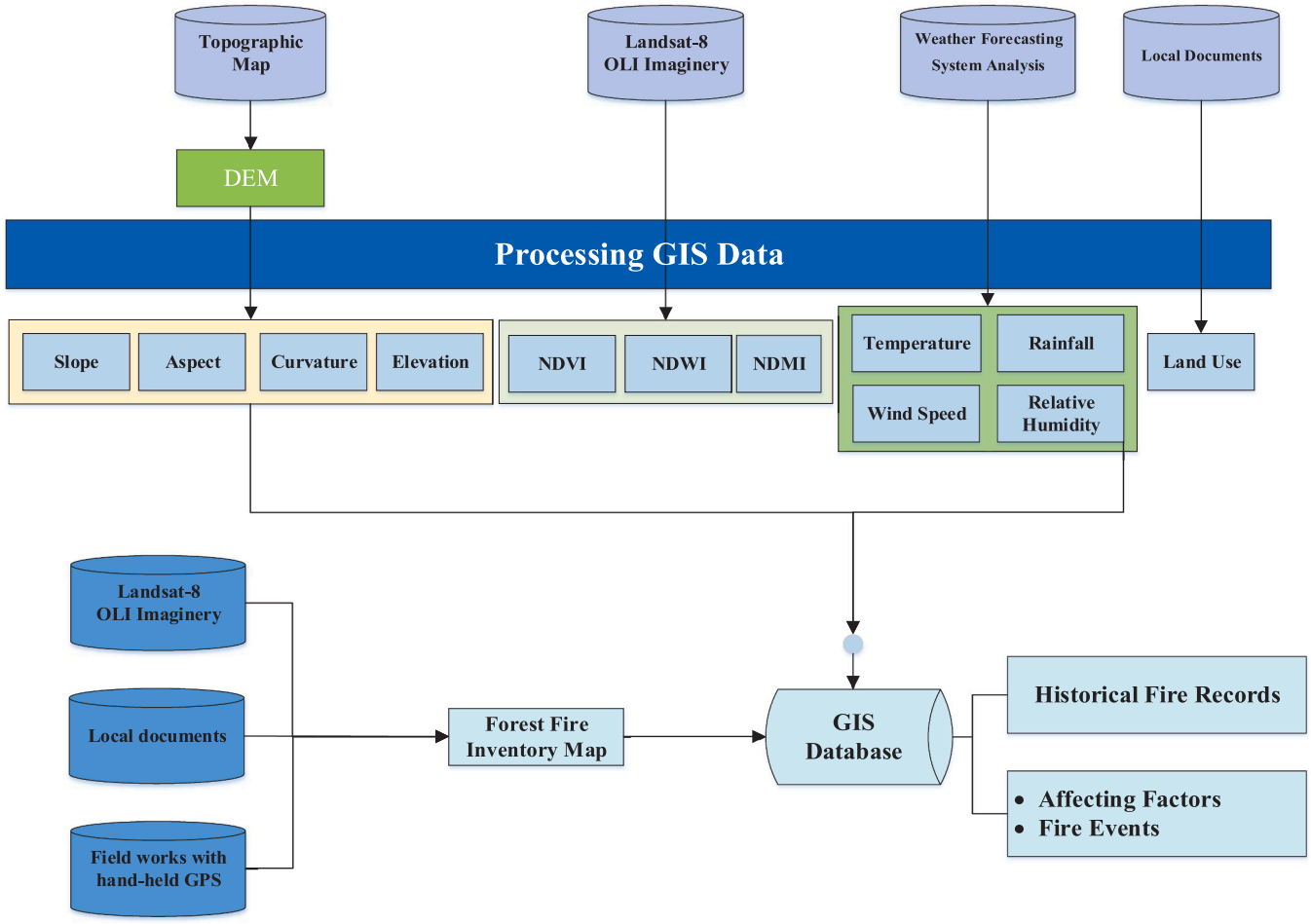

Fig. 5. The established forest fire GIS database.

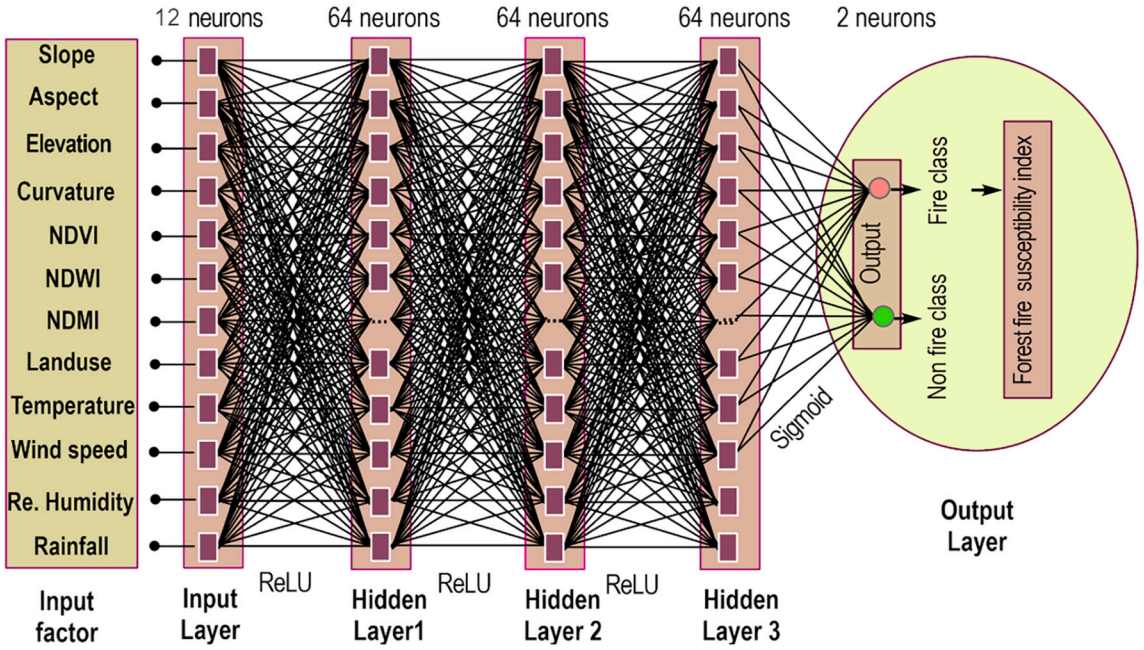

Fig. 6. The proposed Deep-NC model for the forest fire susceptibility in this study.

Finally, the outputs for all the points in the study area can be computed to create a forest fire susceptibility map for the study area.

4.5. Quality assessment of the model

Because the problem of forest fire susceptibility mapping is modeled as a binary classification task, the true positive (TP), the false positive (FP), the false negative (FN), and the true negative (TN) can be computed via comparisons between the actual and predicted class outputs. Based on the four indices of TP, FP, FN, and TN, the Positive predictive value (PPV) or Precision, Negative Predictive Value (NPV), Sensitivity (Sen), Specificity (Spe), and Classification Accuracy Rate (CA) can be computed as follows:

$$PPV = \frac{TP}{TP+FP}; NPV = \frac{TN}{TN+FN}; Sen = \frac{TN}{TN+FN}; Spe = \frac{TN}{TN+FP} \quad (14)$$

$$CA = \frac{TP+TN}{TP+TN+FP+FN} \times 100\% \quad (15)$$

In addition to the above indices, the Receiver operating characteristic (ROC) curve (van Erkel and Pattynama, 1998) and the Kappa index (McHugh, 2012) are often used to evaluate the predictive capability of deep neural network-based classifiers (Hoang et al., 2018b; Nhu et al., 2020).

5. Results and discussion

5.1. Predictive importance of the wildfire driving factors

The predictive importance of each driving factor is shown in Table 1. The result shows that NDVI, NDWI, and NDMI have the highest predictive values. The average impurity decrease (AVID) are 5.65, 2.28, and 1.31, respectively. They are followed by humidity (1.00), temperature (1.00), wind speed (0.91), land use (0.85), rainfall (0.84), and elevation (0.81) (Table 1). The result is in line with the finding in Tien Bui et al. (2017), in which NDVI is the most important factor. Herein, NDVI is associated with a tree cover that affects fuel load variability, a major factor controlling the firing mechanism. In contrast, slope, curvature, and aspect have the lowest predictive values; however, the AVID value of 0.75 for these factors is still useful for predicting wildfire in this research. Overall, all factors are considered for the modeling process.

5.2. Model performance and evaluation

The structure of the Deep-NC model is shown in Fig. 6. The model consists of 206 neurons, which were organized in five layers, namely, one input layer, three hidden layers, and one output layer. A total of 13,377 weights of the Deep-NC model were optimized by the Adam algorithm through the training process, and the result is shown in Table 2 and Fig. 7a. It can be observed that the Deep-NC model has an excellent performance where CA and Kappa values are 95.40% and 0.908, respectively. In addition, the AUC value of 0.983 indicates that the model attained a high global performance. The sensitivity is 92.86%, the specificity is 98.26%, and the Kappa index is 0.908 indicating a high degree-of-fit between the training dataset and the estimated wildfires of the model. Thus, the Adam algorithm is capable of optimizing the weights of the model for the training data set at hand.

Using the validation dataset, the prediction capability of the Deep-NC model was validated, and the result is shown in Table 2 and Fig. 7b. It could be observed that AUC is 0.894, denoting that the global prediction capability is 89.4%. The CA of 81.5% indicates a high classification result of the model, whereas Kappa index of 0.630 denotes a satisfying result.

The validity of the Deep-NC model was further assessed by comparing to those of the Support Vector Machine model (AUC = 0.786), the Relevance Vector Machine model (AUC = 0.793), and the Random Forest model (AUC = 0.790), which were carried out in the previous works of Le et al. (2020). The AUC value of 0.894 of the proposed Deep-NC model indicates that its prediction performance is better than those of the above mentioned models.

5.3. Evaluation of the deep-NC model with different optimization algorithms

Among the employed performance measurement metrics, the AUC index can reflect most accurately the predictive capability of a classifier. Hence, this measurement index is used to evaluate the performance of the proposed Deep-NC model optimized by different algorithms. Table 3 shows the prediction performance of the Adam optimized Deep-NC model using ten random sampling cases as suggested by Nhu et al. (2020). The AUC index in Sample 1 has the highest value (0.933), and that of Sample 2 (0.817) has the lowest value. The average performance of the Adam optimized Deep-NC model is 0.893.

The prediction performance of the SGD optimized Deep-NC model with ten random sampling cases is shown in Table 4. Herein, Sample 5 has the highest AUC value (0.858), whereas Sample 1 has the lowest AUC value (0.807). The average AUC value of the SGD optimized Deep-NC is 0.839. The performances of the RMSprop optimized Deep-NC and Adadelta optimized Deep-NC models are reported in Table 5 and Table 6, respectively. The average performances of these two models are 0.822 and 0.828, respectively. Thus, it can be concluded that the Adam optimized Deep-NC model has achieved the highest accuracy for forest fire prediction with an average AUC value of 0.893.

5.4. Generation of a forest fire danger map

Since the Deep-NC model is capable of providing the high prediction capability of forest fire occurrence, the model was then used to calculate wildfire danger indices for the whole province. The predictive outcomes are transformed into a raster format and opened in ArcGIS. Subsequently, the forest fire susceptibility map (Fig. 8) was derived and visualized with six categories, namely, No forest fire (0–0.086), Very low (0.087–0.282), Low (0.283–0.498), Moderate (0.499–0.710), High

Table 1
Predictive importance of the wildfire driving factors.

Driving factor	Average impurity decrease	Number of nodes used	Ranking
NDVI	5.65	21,255	1
NDWI	2.28	24,352	2
NDMI	1.31	35,128	3
Humidity (%)	1.00	21,919	4
Temperature (°)	1.00	23,845	5
Wind speed (m/s)	0.91	27,402	6
Land use	0.85	35,785	7
Rainfall (mm)	0.84	30,147	8
Elevation (m)	0.81	46,863	9
Slope (°)	0.75	59,574	10
Curvature	0.75	52,101	11
Aspect	0.75	72,394	12

Table 2
Performance of the proposed Deep-NC model.

Metrics	Training dataset	Validation dataset
TP	1742	673
TN	1637	564
FP	29	86
FN	134	195
PPV (%)	98.36	88.7
NPV (%)	92.43	74.3
Sensitivity (%)	92.86	77.5
Specificity (%)	98.26	86.8
CA (%)	95.40	81.5
Kappa	0.908	0.630

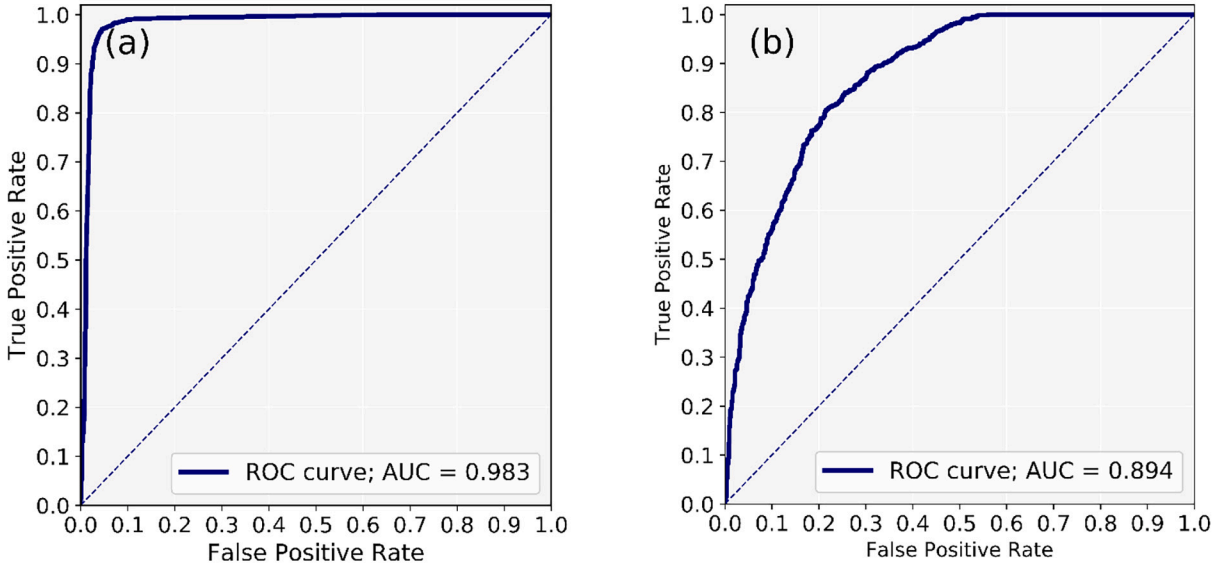

Fig. 7. ROC curve and AUC of the Deep-NC model using (a) the training dataset and (b) the validation dataset.

Table 3
Prediction performance of the Adam optimized Deep-NC model with ten random sampling cases.

Statistical metrics	Ten random sampling cases										Statistics			
	1	2	3	4	5	6	7	8	9	10	Min	Max	Mean	STD
TP	642	570	571	589	639	640	593	658	661	662	570	662	622.5	35.58
TN	661	537	586	615	584	592	636	600	613	623	537	661	604.7	31.94
FP	117	189	188	170	120	119	166	101	98	97	97	189	136.5	35.58
FN	98	222	173	144	175	167	123	159	146	136	98	222	154.3	31.94
PPV	84.58	75.10	75.23	77.60	84.19	84.32	78.13	86.69	87.09	87.22	75.10	87.22	82.02	4.69
NPV	87.09	70.75	77.21	81.03	76.94	78.00	83.79	79.05	80.76	82.08	70.75	87.09	79.67	4.21
Sen	86.76	71.97	76.75	80.35	78.50	79.31	82.82	80.54	81.91	82.96	71.97	86.76	80.19	3.79
Spe	84.96	73.97	75.71	78.34	82.95	83.26	79.30	85.59	86.22	86.53	73.97	86.53	81.68	4.32
CA	85.84	72.92	76.22	79.31	80.57	81.16	80.96	82.87	83.93	84.65	72.92	85.84	80.84	3.74
AUC	0.933	0.817	0.859	0.883	0.884	0.904	0.897	0.906	0.921	0.926	0.817	0.933	0.893	0.033

Table 4
Prediction performance of the SGD optimized Deep-NC model with ten random sampling cases.

Statistical metrics	Ten random sampling cases										Statistics			
	1	2	3	4	5	6	7	8	9	10	Min	Max	Mean	STD
TP	663	655	688	675	658	684	683	719	612	651	612	719	668.8	26.91
TN	462	500	461	465	530	478	486	450	546	532	450	546	491	32.56
FP	96	104	71	84	101	75	76	40	147	108	40	147	90.2	26.91
FN	297	259	298	294	229	281	273	309	213	236	213	309	268.9	31.52
PPV	87.35	86.30	90.65	88.93	86.69	90.12	89.99	94.73	80.63	85.77	80.63	94.73	88.12	3.55
NPV	60.87	65.88	60.74	61.26	69.83	62.98	64.03	59.29	71.94	69.27	59.29	71.94	64.61	4.19
Sen	69.06	71.66	69.78	69.66	74.18	70.88	71.44	69.94	74.18	73.39	69.06	74.18	71.42	1.82
Spe	82.80	82.78	86.65	84.70	83.99	86.44	86.48	91.84	78.79	83.13	78.79	91.84	84.76	3.26
CA	74.11	76.09	75.69	75.10	78.26	76.55	77.01	77.01	76.28	77.47	74.11	78.26	76.36	1.14
AUC	0.807	0.831	0.844	0.831	0.858	0.846	0.844	0.832	0.842	0.855	0.807	0.858	0.839	0.014

(0.711–0.894), and Very high (0.895–1) using the Natural Break method in ArcGIS 10.6 (Bui et al., 2017).

A visual interpretation of the wildfire danger map in ArcGIS shows that very high probabilities of wildfire are at the forests of Ia Grai, Chu Pah, Duc Co, Chu Prong, Ia Pa, and Dak Doa. In these districts, a total number of 8 wildfire events occurred only in 2019, destroying a total amount of 91.35 ha of forests. Therefore, these areas should receive more attention when designing measures for forest prevention and control. In contrast, forest areas in Mang Yang, Chu Se, Phu Thien, and Ayun Pa have a lower probability of wildfire (Fig. 8) due to new-planted forests with low fuel accumulation.

6. Concluding remarks

This work proposed and validated a new approach for the spatial prediction of wildfire danger using deep neural computing with four different optimization algorithms: SGD, RMSProp, Adaptive Adam, and Adadelta. Deep neural computing (Deep-NC) is a sub-branch of ML, which has proven to be very promising in environmental modeling; however, it has not been yet explored for wildfire study. A tropical forest database at the Central Highland (Vietnam) with 12 driving factors and 2530 historical wildfire locations was used to train and verify the proposed models. Based on the findings, some conclusions are given below:

Table 5
Prediction performance of the RMSprop optimized Deep-NC model with ten random sampling cases.

Statistical metrics	Ten random sampling cases										Statistics			
	1	2	3	4	5	6	7	8	9	10	Min	Max	Mean	STD
TP	571	516	493	696	568	528	585	618	611	698	493	698	588.4	66.10
TN	545	578	602	434	563	577	530	510	520	419	419	602	527.8	57.45
FP	188	243	266	63	191	231	174	141	148	61	61	266	170.6	66.10
FN	214	181	157	325	196	182	229	249	239	340	157	340	231.2	57.45
PPV	75.23	67.98	64.95	91.70	74.84	69.57	77.08	81.42	80.50	91.96	64.95	91.96	77.52	8.71
NPV	71.81	76.15	79.31	57.18	74.18	76.02	69.83	67.19	68.51	55.20	55.20	79.31	69.54	7.57
Sen	72.74	74.03	75.85	68.17	74.35	74.37	71.87	71.28	71.88	67.24	67.24	75.85	72.18	2.61
Spe	74.35	70.40	69.35	87.32	74.67	71.41	75.28	78.34	77.84	87.29	69.35	87.32	76.63	6.02
CA	73.52	72.07	72.13	74.44	74.51	72.79	73.45	74.31	74.51	73.58	72.07	74.51	73.53	0.89
AUC	0.821	0.828	0.840	0.806	0.836	0.819	0.825	0.811	0.817	0.814	0.806	0.840	0.822	0.010

Table 6
Prediction performance of the Adadelta optimized Deep-NC model with ten random sampling cases.

Statistical metrics	Ten random sampling cases										Statistics			
	1	2	3	4	5	6	7	8	9	10	Min	Max	Mean	STD
TP	588	589	540	614	669	621	632	668	729	701	540	729	635.1	54.25
TN	541	538	565	517	497	521	507	474	405	429	405	565	499.4	47.83
FP	171	170	219	145	90	138	127	91	30	58	30	219	123.9	54.25
FN	218	221	194	242	262	238	252	285	354	330	194	354	259.6	47.83
PPV	77.47	77.60	71.15	80.90	88.14	81.82	83.27	88.01	96.05	92.36	71.15	96.05	83.68	7.15
NPV	71.28	70.88	74.44	68.12	65.48	68.64	66.80	62.45	53.36	56.52	53.36	74.44	65.80	6.30
Sen	72.95	72.72	73.57	71.73	71.86	72.29	71.49	70.09	67.31	67.99	67.31	73.57	71.20	1.99
Spe	75.98	75.99	72.07	78.10	84.67	79.06	79.97	83.89	93.10	88.09	72.07	93.10	81.09	6.02
CA	74.37	74.24	72.79	74.51	76.81	75.23	75.03	75.23	74.70	74.44	72.79	76.81	74.74	0.96
AUC	0.825	0.831	0.831	0.818	0.847	0.836	0.826	0.816	0.821	0.827	0.816	0.847	0.828	0.009

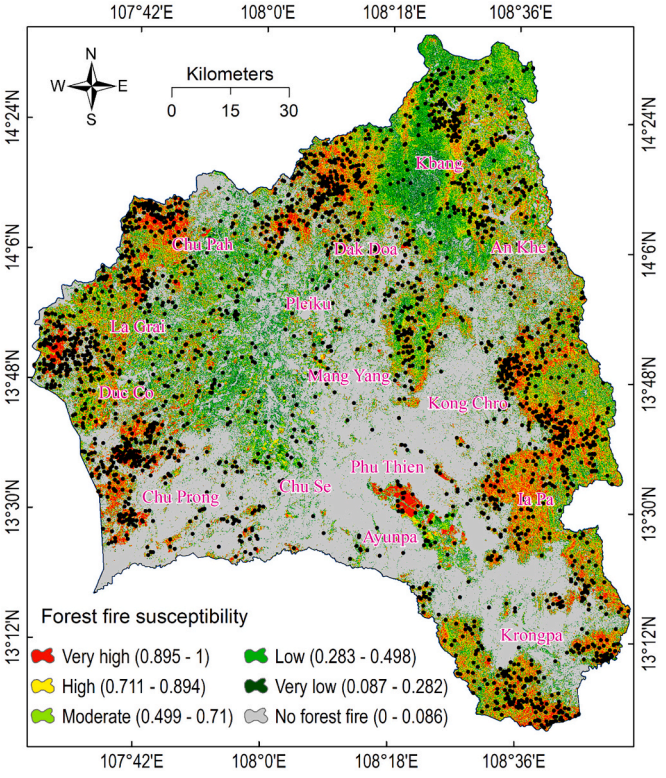

Fig. 8. Wildfire danger map for the study area using the Deep-NC model.

- The Deep-NC model's behavior for predicting wildfire is strongly dependent on how its weights were updated. Among the four optimization algorithms, Adam algorithm has the best performance, whereas there is no significant difference in the performance of the models using the other optimization algorithms.
- The performance of the Deep-NC models is higher than those of benchmarks, namely, Relevance Vector Machines, Support Vector Machines, and Random Forests. Thus, Deep-NC is a promising tool that should be considered for predicting wildfire danger.
- One of the difficulties in designing Deep-NC models is the determination of the number of hidden layers and the number of neurons for each of them. In this work, although three hidden layers with 64 neurons each were utilized based on a suggestion in Tien Bui et al. (2020), there is no guarantee that this is an optimal structure of the Deep-NC model. Therefore, the performance of the Deep-NC model could be improved by investigating a more optimal structure for the model.
- The high performance of the Deep-NC model in this work is adequate for producing the wildfire danger map, which is beneficial for provincial authorities in forest prevention and control.
- Future works could focus on how to optimize the structure of Deep-NC models for wildfire studies. Also, new ML optimization algorithms, e.g., Coronavirus Optimization Algorithm (Martínez-Álvarez et al., 2020) and Balancing composite motion algorithm (Le-Duc et al., 2020), should be utilized for training Deep-NC models.

Declaration of Competing Interest

None.

Acknowledgment

This research is funded by Vietnam National Foundation for Science and Technology Development (NAFOSTED) under grant number 105.08-2018.09.

References

Barrera, F.D.L., Barraza, F., Favier, P., Ruiz, V., Quense, J., 2018. Megafires in Chile 2017: monitoring multiscale environmental impacts of burned ecosystems. Sci. Total Environ. 637, 1526–1536.
Akinola, O., Adegoke, J., 2019. Assessment of forest fire vulnerability zones in Missouri, United States of America. Int.J. Sustain. Dev. World Ecol. 26, 251–257.
Alexandridis, A., Vakalis, D., Siettos, C.I., Bafas, G.V., 2008. A cellular automata model for forest fire spread prediction: the case of the wildfire that swept through Spetses Island in 1990. Appl. Math. Comput. 204, 191–201.
Bennie, J., Huntley, B., Wiltshire, A., Hill, M.O., Baxter, R., 2008. Slope, aspect and climate: spatially explicit and implicit models of topographic microclimate in chalk grassland. Ecol. Model. 216, 47–59.
Bolton, T., Zanna, L., 2019. Applications of deep learning to ocean data inference and subgrid parameterization. J. Adv. Model. Earth Syst. 11, 376–399.
Brown, J.L., 2014. SDM toolbox: a python-based GIS toolkit for landscape genetic, biogeographic and species distribution model analyses. Methods Ecol. Evol. 5, 694–700.
Brunello, C.F., Andermann, C., Helle, G., Comiti, F., Tonon, G., Tiwari, A., Hovius, N., 2019. Hydroclimatic seasonality recorded by tree ring δ18O signature across a Himalayan altitudinal transect. Earth Planet. Sci. Lett. 518, 148–159.
Bui, D.T., Pradhan, B., Lofman, O., Revhaug, I., Dick, O.B., 2012. Landslide susceptibility assessment in the Hoa Binh province of Vietnam: a comparison of the Levenberg–Marquardt and Bayesian regularized neural networks. Geomorphology 171, 12–29.
Bui, D.T., Bui, Q.-T., Nguyen, Q.-P., Pradhan, B., Nampak, H., Trinh, P.T., 2017. A hybrid artificial intelligence approach using GIS-based neural-fuzzy inference system and particle swarm optimization for forest fire susceptibility modeling at a tropical area. Agric. For. Meteorol. 233, 32–44.
Carlson, T.N., Ripley, D.A., 1997. On the relation between NDVI, fractional vegetation cover, and leaf area index. Remote Sens. Environ. 62, 241–252.
Cary, G.J., Flannigan, M.D., Keane, R.E., Bradstock, R.A., Davies, I.D., Lenihan, J.M., Li, C., Logan, K.A., Parsons, R.A., 2009. Relative importance of fuel management, ignition management and weather for area burned: evidence from five landscape–fire–succession models. Int. J. Wildland Fire 18, 147–156.
CGIAR, 2016. The Drought Crisis in the Central Highlands of Vietnam: Assessment Report, 36. CGIAR Research Centers in Southeast Asia.
Chen, B.-X., Sun, Y.-F., Zhang, H.-B., Han, Z.-H., Wang, J.-S., Li, Y.-K., Yang, X.-L., 2018. Temperature change along elevation and its effect on the alpine timberline tree growth in the southeast of the Tibetan Plateau. Adv. Clim. Chang. Res. 9, 185–191.
Chollet, F., 2018. Keras: The Python Deep Learning Library (Astrophysics Source Code Library).
Chuvieco, E., Aguado, I., Yebra, M., Nieto, H., Salas, J., Martín, M.P., Vilar, L., Martínez, J., Martín, S., Ibarra, P., 2010a. Development of a framework for fire risk assessment using remote sensing and geographic information system technologies. Ecol. Model. 221, 46–58.
Chuvieco, E., Aguado, I., Yebra, M., Nieto, H., Salas, J., Martín, M.P., Vilar, L., Martínez, J., Martín, S., Ibarra, P., de la Riva, J., Baeza, J., Rodríguez, F., Molina, J. R., Herrera, M.A., Zamora, R., 2010b. Development of a framework for fire risk assessment using remote sensing and geographic information system technologies. Ecol. Model. 221, 46–58.
Chuvieco, E., Aguado, I., Jurdao, S., Pettinari, M.L., Yebra, M., Salas, J., Hantson, S., de la Riva, J., Ibarra, P., Rodrigues, M., 2014. Integrating geospatial information into fire risk assessment. Int. J. Wildland Fire 23, 606–619.
Claverie, M., Ju, J., Masek, J.G., Dungan, J.L., Vermote, E.F., Roger, J.-C., Skakun, S.V., Justice, C., 2018. The harmonized Landsat and Sentinel-2 surface reflectance data set. Remote Sens. Environ. 219, 145–161.
Çolak, E., Sunar, F., 2020a. Evaluation of forest fire risk in the Mediterranean Turkish forests: a case study of Menderes region, Izmir. Int. J. Disaster Risk Reduct. 45, 101479.
Çolak, E., Sunar, F., 2020b. Evaluation of forest fire risk in the Mediterranean Turkish forests: a case study of Menderes region, Izmir. Int. J. Disaster Risk Reduct. 101479.
Di Virgilio, G., Evans, J.P., Blake, S.A., Armstrong, M., Dowdy, A.J., Sharples, J., McRae, R., 2019. Climate change increases the potential for extreme wildfires. Geophys. Res. Lett. 46, 8517–8526.
Dupuy, J.-L., Maréchal, J., 2011. Slope effect on laboratory fire spread: contribution of radiation and convection to fuel bed preheating. Int. J. Wildland Fire 20, 289–307.
van Erkel, A.R., Pattynama, P.M.T., 1998. Receiver operating characteristic (ROC) analysis: basic principles and applications in radiology. Eur. J. Radiol. 27, 88–94.
Gamon, J.A., Field, C.B., Goulden, M.L., Griffin, K.L., Hartley, A.E., Joel, G., Peñuelas, J., Valentini, R., 1995. Relationships between NDVI, canopy structure, and photosynthesis in three Californian vegetation types. Ecol. Appl. 5, 28–41.
Ganapathi Subramanian, S., Crowley, M., 2018. Using spatial reinforcement learning to build forest wildfire dynamics models from satellite images. Front. ICT 5, 6.
General Statistic Office, 2018. Statistical Yearbook of Vietnam, Hanoi.
Gibson, R., Danaher, T., Hehir, W., Collins, L., 2020. A remote sensing approach to mapping fire severity in south-eastern Australia using sentinel 2 and random forest. Remote Sens. Environ. 240, 111702.
Gill, A.M., Stephens, S.L., Cary, G.J., 2013. The worldwide "wildfire" problem. Ecol. Appl. 23, 438–454.
Gillett, N.P., Weaver, A.J., Zwiers, F.W., Flannigan, M.D., 2004. Detecting the effect of climate change on Canadian forest fires. Geophys. Res. Lett. 31.
Goodfellow, I., Bengio, Y., Courville, A., 2016. Deep Learning (Adaptive Computation and Machine Learning Series). The MIT Press. ISBN-10: 0262035618.
GSO, 2019. General Statistics Office of Vietnam. http://www.gso.gov.vn.
Guo, F., Su, Z., Wang, G., Sun, L., Lin, F., Liu, A., 2016a. Wildfire ignition in the forests of southeast China: identifying drivers and spatial distribution to predict wildfire likelihood. Appl. Geogr. 66, 12–21.
Guo, Y., Liu, Y., Oerlemans, A., Lao, S., Wu, S., Lew, M.S., 2016b. Deep learning for visual understanding: a review. Neurocomputing 187, 27–48.
Heaton, J., 2015. Artificial Intelligence for Humans, Volume 3 Deep Learning and Neural Networks. Heaton Research, Inc., United States.
Hernandez-Leal, P., Arbelo, M., Gonzalez-Calvo, A., 2006. Fire risk assessment using satellite data. Adv. Space Res. 37, 741–746.
Hilton, J., Miller, C., Sharples, J., Sullivan, A., 2017. Curvature effects in the dynamic propagation of wildfires. Int. J. Wildland Fire 25, 1238–1251.
Hoa, P.V., Giang, N.V., Binh, N.A., Hai, L.V.H., Pham, T.-D., Hasanlou, M., Tien Bui, D., 2019. Soil salinity mapping using SAR sentinel-1 data and advanced machine learning algorithms: a case study at Ben Tre Province of the Mekong River Delta (Vietnam). Remote Sens. 11, 128.
Hoang, N.-D., Nguyen, Q.-L., Tran, V.-D., 2018a. Automatic recognition of asphalt pavement cracks using metaheuristic optimized edge detection algorithms and convolution neural network. Autom. Constr. 94, 203–213.
Hoang, N.-D., Le, V.-H., Tien Bui, D., 2018b. GIS-based spatial prediction of tropical forest fire danger using a new hybrid machine learning method. Ecol. Inform. 48, 104–116.
Jiang, G.Q., Xu, J., Wei, J., 2018. A deep learning algorithm of neural network for the parameterization of typhoon-ocean feedback in typhoon forecast models. Geophys. Res. Lett. 45, 3706–3716.
Johansson, T., Gibb, H., Hjältén, J., Dynesius, M., 2017. Soil humidity, potential solar radiation and altitude affect boreal beetle assemblages in dead wood. Biol. Conserv. 209, 107–118.
Kim, P., 2017. MatLab Deep Learning with Machine Learning. Neural Networks and Artificial Intelligence. Apress.
Kingma, D.P., Ba, J., 2015a. Adam: A method for stochastic optimization. In: Proceedings of the 3rd International Conference on Learning Representations (ICLR), San Diego, p. 2015.
Kingma, D.P., Ba, J.L., 2015b. Adam: A method for stochastic optimization. In: Advanced Seminar in Deep Learning (#67679). The Hebrew University of Jerusalem.
Kissinger, G., Gupta, A., Mulder, I., Unterstell, N., 2019. Climate financing needs in the land sector under the Paris agreement: an assessment of developing country perspectives. Land Use Policy 83, 256–269.
Koubarakis, M., Bereta, K., Papadakis, G., Savva, D., Stamoulis, G., 2017. Big, linked geospatial data and its applications in earth observation. IEEE Internet Comput. 21, 87–91.
Lacroix, K., Gifford, R., Rush, J., 2020. Climate change beliefs shape the interpretation of forest fire events. Clim. Chang. 159, 103–120.
Le, H.-V., Bui, Q., Bui, D.T., Tran, H., Hoang, N., 2020. A hybrid intelligence system based on relevance vector machines and imperialist competitive optimization for modelling Forest fire danger using GIS. J. Environ. Inf. 36 (1), 43–57. https://doi.org/10.3808/jei.201800404.
LeCun, Y., Bengio, Y., Hinton, G., 2015. Deep learning. Nature 521, 436–444.
Le-Duc, T., Nguyen, Q.-H., Nguyen-Xuan, H., 2020. Balancing composite motion optimization. Inf. Sci. 520, 250–270.
Liu, Y., Goodrick, S.L., Stanturf, J.A., 2013. Future U.S. wildfire potential trends projected using a dynamically downscaled climate change scenario. For. Ecol. Manag. 294, 120–135.
Liu, Y., Hill, M.J., Zhang, X., Wang, Z., Richardson, A.D., Hufkens, K., Filippa, G., Baldocchi, D.D., Ma, S., Verfaillie, J., 2017. Using data from Landsat, MODIS, VIIRS and PhenoCams to monitor the phenology of California oak/grass savanna and open grassland across spatial scales. Agric. For. Meteorol. 237, 311–325.
Lozano, O.M., Salis, M., Ager, A.A., Arca, B., Alcasena, F.J., Monteiro, A.T., Finney, M.A., Del Giudice, L., Scoccimarro, E., Spano, D., 2017. Assessing climate change impacts on wildfire exposure in Mediterranean areas. Risk Anal. 37, 1898–1916.
Martínez-Álvarez, F., Asencio-Cortés, G., Torres, J., Gutiérrez-Avilés, D., Melgar-García, L., Pérez-Chacón, R., Rubio-Escudero, C., Riquelme, J.C., Troncoso, A., 2020. Coronavirus optimization algorithm: a bioinspired metaheuristic based on the COVID-19 propagation model. Big Data 8, 308–322.
Matin, M.A., Chitale, V.S., Murthy, M.S., Uddin, K., Bajracharya, B., Pradhan, S., 2017. Understanding forest fire patterns and risk in Nepal using remote sensing, geographic information system and historical fire data. Int. J. Wildland Fire 26, 276–286.
McFayden, C.B., Woolford, D.G., Stacey, A., Boychuk, D., Johnston, J.M., Wheatley, M.J., Martell, D.L., 2020. Risk assessment for wildland fire aerial detection patrol route planning in Ontario, Canada. Int. J. Wildland Fire 29, 28–41.
McFeeters, S.K., 1996. The use of the Normalized Difference Water Index (NDWI) in the delineation of open water features. Int. J. Remote Sens. 17, 1425–1432.
McHugh, M.L., 2012. Interrater reliability: the kappa statistic. Biochem. Med. (Zagreb) 22, 276–282.
Mermoz, M., Kitzberger, T., Veblen, T.T., 2005. Landscape influences on occurrence and spread of wildfires in Patagonian forests and shrublands. Ecology 86, 2705–2715.
Mhawej, M., Faour, G., Adjizian-Gerard, J., 2015. Wildfire likelihood's elements: a literature review. Challenges 6, 282–293.

Mhawej, M., Faour, G., Abdallah, C., Adjizian-Gerard, J., 2016. Towards an establishment of a wildfire risk system in a Mediterranean country. Ecol. Inform. 32, 167–184.
Mondal, P., McDermid, S.S., Qadir, A., 2020. A reporting framework for sustainable development goal 15: multi-scale monitoring of forest degradation using MODIS, Landsat and sentinel data. Remote Sens. Environ. 237, 111592.
Moreno, M.V., Conedera, M., Chuvieco, E., Pezzatti, G.B., 2014. Fire regime changes and major driving forces in Spain from 1968 to 2010. Environ. Sci. Pol. 37, 11–22.
Naderpour, M., Rizeei, H.M., Khakzad, N., Pradhan, B., 2019. Forest fire induced Natech risk assessment: a survey of geospatial technologies. Reliab. Eng. Syst. Saf. 191, 106558.
Nhu, V.-H., Hoang, N.-D., Nguyen, H., Ngo, P.T.T., Thanh Bui, T., Hoa, P.V., Samui, P., Tien Bui, D., 2020. Effectiveness assessment of Keras based deep learning with different robust optimization algorithms for shallow landslide susceptibility mapping at tropical area. CATENA 188, 104458.
Opitz, T., Bonneu, F., Gabriel, E., 2020. Point-process based Bayesian modeling of space–time structures of forest fire occurrences in Mediterranean France. Spat. Stat. 100429.
Peng, Y., Wang, Y., 2019. Real-time forest smoke detection using hand-designed features and deep learning. Comput. Electron. Agric. 167, 105029.
Pereira, M.G., Parente, J., Amraoui, M., Oliveira, A., Fernandes, P.M., 2020. The role of weather and climate conditions on extreme wildfires. In: Extreme Wildfire Events and Disasters. Elsevier, pp. 55–72.
Pourghasemi, H.R., Kariminejad, N., Amiri, M., Edalat, M., Zarafshar, M., Blaschke, T., Cerda, A., 2020. Assessing and mapping multi-hazard risk susceptibility using a machine learning technique. Sci. Rep. 10, 1–11.
Pourtaghi, Z.S., Pourghasemi, H.R., Aretano, R., Semeraro, T., 2016. Investigation of general indicators influencing on forest fire and its susceptibility modeling using different data mining techniques. Ecol. Indic. 64, 72–84.
Ross, Z.E., Yue, Y., Meier, M.A., Hauksson, E., Heaton, T.H., 2019. PhaseLink: a deep learning approach to seismic phase association. J. Geophys. Res. Solid Earth 124, 856–869.
Roy, D.P., Huang, H., Boschetti, L., Giglio, L., Yan, L., Zhang, H.H., Li, Z., 2019. Landsat-8 and Sentinel-2 burned area mapping-a combined sensor multi-temporal change detection approach. Remote Sens. Environ. 231, 111254.
Ruder, S., 2017. An overview of gradient descent optimization algorithms. arXiv: 1609.04747v2 [cs.LG].
Sankaranarayanan, S., Prabhakar, M., Satish, S., Jain, P., Ramprasad, A., Krishnan, A., 2020. Flood prediction based on weather parameters using deep learning. J. Water Clim. Change 11 (4), 1766–1783. https://doi.org/10.2166/wcc.2019.321.
Silva, S.J., Heald, C.L., Ravela, S., Mammarella, I., Munger, J.W., 2019. A deep learning parameterization for ozone dry deposition velocities. Geophys. Res. Lett. 46, 983–989.
Singaravel, S., Suykens, J., Geyer, P., 2018. Deep-learning neural-network architectures and methods: using component-based models in building-design energy prediction. Adv. Eng. Inform. 38, 81–90.
Skansi, S., 2018. Introduction to Deep Learning - From Logical Calculus to Artificial Intelligence. Springer International Publishing, United States. https://doi.org/10.1007/978-3-319-73004-2.
Soille, P., Burger, A., De Marchi, D., Kempeneers, P., Rodriguez, D., Syrris, V., Vasilev, V., 2018. A versatile data-intensive computing platform for information retrieval from big geospatial data. Futur. Gener. Comput. Syst. 81, 30–40.
Sugomori, Y., Kaluza, B., Soares, F.M., Souza, A.M.F., 2017. Deep Learning - Practical Neural Networks with Java. Packt Publishing Limited, United Kingdom.
Sutton, W.R., Srivastava, J.P., Rosegrant, M., Thurlow, J., Vasileiou, I., 2019. Striking a Balance: Managing El Niño and La Niña in Myanmar's Agriculture. World Bank.
Taufik, M., Torfs, P.J., Uijlenhoet, R., Jones, P.D., Murdiyarso, D., Van Lanen, H.A., 2017. Amplification of wildfire area burnt by hydrological drought in the humid tropics. Nat. Clim. Chang. 7, 428–431.
Tehrany, M.S., Jones, S., Shabani, F., Martínez-Álvarez, F., Bui, D.T., 2019. A novel ensemble modeling approach for the spatial prediction of tropical forest fire susceptibility using logitboost machine learning classifier and multi-source geospatial data. Theor. Appl. Climatol. 137, 637–653.
Teodoro, A., Amaral, A., 2019. A statistical and spatial analysis of Portuguese Forest fires in summer 2016 considering Landsat 8 and sentinel 2A data. Environments 6, 36.
Thach, N.N., Ngo, D.B.-T., Xuan-Canh, P., Hong-Thi, N., Thi, B.H., Nhat-Duc, H., Dieu, T. B., 2018. Spatial pattern assessment of tropical forest fire danger at Thuan Chau area (Vietnam) using GIS-based advanced machine learning algorithms: a comparative study. Ecol. Inform. 46, 74–85.
Tieleman, T., Hinton, G., 2012. Lecture 6.5 - RMSProp. COURSERA: Neural Networks for Machine Learning. Technical report.
Tien Bui, D., Hoang, N.-D., Martínez-Álvarez, F., Ngo, P.-T.T., Hoa, P.V., Pham, T.D., Samui, P., Costache, R., 2020. A novel deep learning neural network approach for predicting flash flood susceptibility: a case study at a high frequency tropical storm area. Sci. Total Environ. 701, 134413.
Tucker, C.J., 1979. Red and photographic infrared linear combinations for monitoring vegetation. Remote Sens. Environ. 8, 127–150.
Van, N.K., Ly, P.T., Hong, N.T., 2014. Bioclimatic map of Tay Nguyen at scale 1: 250,000 for setting up sustainable ecological economic models. Viet. J. Earth Sci. 36, 504–514.
Viedma, O., Moreno, J.M., Güngöroglu, C., Cosgun, U., Kavgacı, A., 2017. Recent land-use and land-cover changes and its driving factors in a fire-prone area of southwestern Turkey. J. Environ. Manag. 197, 719–731.
Wang, Y., Dang, L., Ren, J., 2019. Forest fire image recognition based on convolutional neural network. J. Algorith. Comput. Technol. 13 (1748302619887689).
Wibisana, A.G., 2019. The many faces of strict liability in Indonesia's wildfire litigation. Rev. Eur. Comp. Int. Environ. Law 28, 185–196.
Wilson, E.H., Sader, S.A., 2002. Detection of forest harvest type using multiple dates of Landsat TM imagery. Remote Sens. Environ. 80, 385–396.
Wu, Z., Zhou, Y., Wang, H., Jiang, Z., 2020. Depth prediction of urban flood under different rainfall return periods based on deep learning and data warehouse. Sci. Total Environ. 716, 137077.
You, W., Lin, L., Wu, L., Ji, Z., Zhu, J., Fan, Y., He, D., 2017. Geographical information system-based forest fire risk assessment integrating national forest inventory data and analysis of its spatiotemporal variability. Ecol. Indic. 77, 176–184.
Zdeborová, L., 2017. Machine learning: new tool in the box. Nat. Phys. 13, 420–421.
Zeiler, M.D., 2012. ADADELTA: An Adaptive Learning Rate Method arXiv:1212.5701 [cs. LG].
Zhang, G., Wang, M., Liu, K., 2019. Forest fire susceptibility Modeling using a convolutional neural network for Yunnan Province of China. Int. J. Disaster Risk Sci. 10, 386–403.